Chemical Science Review and Letters ISSN 2278-6783

Research Article

Electro Analytical and Gravimetrical Investigations on Corrosion Inhibition Properties of Pyridine-Carbaldehyde Derivatives on Carbon Steel

C Sini Varghese[1], K Joby Thomas[1]*, Vinod P Raphael[2] and K.S Shaju[2]

[1]Department of Chemistry, St. Thomas' College (Autonomous) Thrissur, Kerala, India
[2]Department of Chemistry, Govt. Engineering College Thrissur, Keala, India

Abstract

The corrosion inhibition efficiency of 2-Pyridine carbaldehyde oxime 2PCOX and 3-Pyridine carbaldehyde oxime 3PCOX on carbon steel in 1.0 M HCl solution have been investigated using weight loss measurements, electrochemical impedance spectroscopy (EIS) and potentiodynamic polarization studies. The results show that inhibition efficiencies of both oximes increase with increase in concentration. 3PCOX exhibited comparatively good inhibition towards CS corrosion in HCl medium even at low concentrations. The adsorption of inhibitors 2PCOX and 3PCOX on the surfaces of the corroding metal obeys El-Awady and Langmuir adsorption isotherm respectively. Polarization studies revealed that 2PCOX and 3PCOX are mixed type inhibitor. Thermodynamic parameters (K_{ads}, ΔG^0_{ads}) were calculated using adsorption isotherm.

Keywords: Carbon steel, oxime, Corrosion inhibitors, Isotherm

***Correspondence**
Author: K Joby Thomas
Email: drjobythomask@gmail.com

Introduction

The molecules containing heteroatom have many applications in the field of science, especially industries like oil and gas industry. The hetero atoms present in these molecules are of important and are responsible for the corrosion inhibition in acidic media on the metal surface [1-3]. Some recently reported heterocyclic derivatives showed effective inhibition for mild steel (MS), carbon steel (CS), aluminum, copper and zinc in acidic media [4-11].

The study on carbon steel (CS) and copper corrosion has become much important particularly in industrial and academic field. Enormous use of hydrochloric acid for acid pickling, de-scaling and cleaning process of metal surface are the major reasons for the corrosion problems. Increasing efforts have been made to study the corrosion behavior of metals and mechanism of inhibition during the past decade mainly through electrochemical investigations [8, 9]. Limited work has been reported for the corrosion inhibition of compounds derived from pyridine in acid media. The present investigation was undertaken to examine the corrosion inhibition capacity and mechanism of inhibition of oximes derived from pyridine carbaldehyde that is 2PCOX and 3PCOX in 1.0M HCl solution on CS. The study was performed using weight loss measurements, adsorption isotherms, electrochemical impedance spectroscopy (EIS), and potentiodynamic polarization analysis.

Experimental

Inhibitor

The oximes 2PCOX and 3PCOX were prepared by adopting the following procedure. To a 1:2 ratio mixtures of hydroxylamine hydrochloride and sodium acetate in aqueous medium, alcoholic solution of Pyridine-2-carbaldehyde/pyridine-3-carbaldehydewas added with constant stirring, refluxed for 20 minutes and cooled in an ice bath. The separated oxime filtered, washed with alcohol-water mixture (1:1) and dried. **Figure 1** shows the molecular structure of heterocyclic oxime 2PCOX. Anal.calcd for $C_6H_6N_2O$: C, 59.01; H, 4.91; N, 22.95 ; O, 13.12%. Found. C, 58.45; H, 4.54; N, 22.56 ; O, 12.72% ; IR (KBr) : $\nu_{C=N}$ 1593 cm^{-1} . ^{1}Hnmr: δ_{OH} 9.65, $\delta_{CH=N}$ 8.27. ^{13}Cnmr: $\delta_{CH=N}$ 136.82. Mass: M^+ peak and base peak m/z:122. m. p. = 135 ^{0}C. **Figure 2** shows the molecular structure of heterocyclic oxime 3PCOX Anal.calcd for $C_6H_6N_2O$: C, 59.01; H, 4.91; N, 22.95 ; O, 13.12%. Found. C, 58.29; H, 4.44; N, 22.47 ; O, 12.97% ; IR (KBr) : $\nu_{C=N}$ 1633 cm^{-1} . ^{1}Hnmr: δ_{OH} 8.66, $\delta_{CH=N}$ 8.17. ^{13}Cnmr: $\delta_{CH=N}$ 133.74. Mass:M^+ peak and base peak m/z:122. m.p. = 108 ^{0}C;

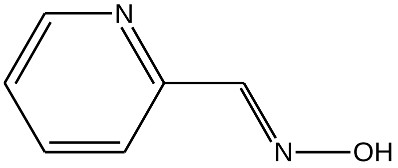

Figure 1 Molecular Structure of 2PCOX

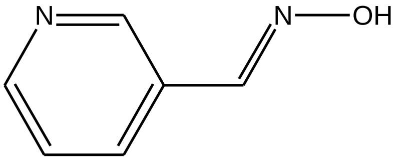

Figure 2 Molecular Structure of 3PCOX

Solutions

The aggressive solutions were prepared by diluting of A. R grade 37% of HCl (Merck) with de-ionized water to obtain 1.0M HCl. Inhibitor solutions were prepared in the range, 0.2mM-1mM in 1.0M HCl.

Weight loss measurements

Carbon steel specimens of dimension 1.5 x 2 x 0.1 cm were cut abraded with various grades of silicon carbide papers (200, 400, 600, 800, 1000, 1200and 2000). The exact area and thickness of each coupon were measured and washed with distilled water containing detergent. Specimens were degreased with acetone and finally dried. After weighing, specimens were immersed in 50ml acid solutions (non-deaerated) at 28 ^{0}C in the absence and presence of the inhibitor, using hooks and fishing lines. Weight loss of metal specimens was noted after 24 hours. The experiments were carried out in duplicate and the average values were reported. The corrosion rate (ν) and percentage of inhibition efficiency (η) were calculated by the following equations [8, 12].

$$\nu = \frac{W}{St} \qquad (1)$$

$$\eta_w\% = \frac{\nu_0 - \nu}{\nu_0} \times 100 \qquad (2)$$

Where W is the average weight loss of coupon, S is the total area of specimens and t is the time of treatment (24 hr). Where ν_0 and ν are the corrosion rates of uninhibited and inhibited specimens respectively.

Electrochemical Impedance Spectroscopy (EIS)

The EIS measurements were performed in a three electrode assembly. Saturated calomel electrode (SCE) was used as the reference electrode. Platinum electrode having 1cm^2 area was taken as counter electrode. Metal specimens with an exposed area of 1cm^2 were used as the working electrode. The EIS experiments were carried out on an Ivium compactstat-e electrochemical system. 1.0M HCl acid was taken as the electrolyte and the working area of the metal specimens were exposed to the electrolyte for 1 h prior to the measurement. EIS measurements were performed at constant potential (OCP) in the frequency range from 1 KHz to 100 mHz with amplitude of 10 mV as excitation signal. The percentage of inhibitions from impedance measurements were calculated using charge transfer resistance values by the following expression [2]:

$$\eta_{EIS}\% = \frac{R_{ct} - R'_{ct}}{R_{ct}} \times 100 \qquad (3)$$

Where, R_{ct} and R'_{ct} are the charge transfer resistances of working electrode with and without inhibitor respectively.

Potentiodynamic polarization

Electrochemical polarization studies of carbon steel specimens in 1.0M HCl with and without inhibitor were performed by recording anodic and cathodic potentiodynamic polarization curves. Polarization plots were obtained in the electrode potential range from -250 to +250 mV Vs corrosion potential (E_{corr}) at a scan rate of 1mV/sec. Tafel polarization analysis were done by extrapolating anodic and cathodic curves to the potential axis to obtain corrosion current densities(I_{corr}). The percentage of inhibition efficiency ($\eta_{pol\%}$) was evaluated from I_{corr} values using the following relation [13]:

$$\eta_{pol}\% = \frac{I_{corr} - I'_{corr}}{I_{corr}} \times 100 \qquad (4)$$

Where, I_{corr} and I'_{corr} are the corrosion current densities of the exposed area of the working electrode in the absence and presence of inhibitor.

From the slope analysis the values of polarization resistance (R_p) in 1.0M HCl solution were obtained. Using the evaluated polarization resistance, the inhibition efficiency was calculated using the relationship

$$\eta_{Rp}\% = \frac{R'_p - R_p}{R'_p} \times 100 \qquad (5)$$

Where, R'_p and R_p are the polarization resistance in the presence and absence of inhibitor respectively [2].

Results and Discussions

Weight loss measurements

Weight loss of carbon steel specimens in 1.0M HCl was determined at 24 h interval in the presence of various concentrations of inhibitor. The corrosion rates and inhibition efficiencies obtained for 2PCOX and 3PCOX for CS specimens for a period of 24 h are listed in **Table 1**. For CS specimens the corrosion rate markedly decreased with increase in inhibitor concentration. About the corrosion behavior of CS specimens, the metal showed low corrosion rate in the presence of 3PCOX, when it was compared with 2PCOX this can be attributed to the surface coverage of the inhibitor molecules on the metal through adsorption [14]. Among the oximes 2PCOX and 3PCOX, former one exhibited lesser inhibition efficiency than latter on CS surface in acidic medium at all concentration. A maximum inhibition efficiency of 68.6% was exhibited by 2PCOX at a concentration 1mM, while 3PCOX showed inhibition efficiency of 85.2% for the same concentration.

Table 1 The corrosion rate of CS and percentage of inhibition efficiency in the presence and absence of 2PCOX and 3PCOX in 1.0M HCl at 28 ^{0}C for 24 h

Conc.	**2PCOX**		**3PCOX**	
(mM)	**ν (mmy^{-1})**	**η_w%**	**ν (mmy^{-1})**	**η_w%**
0	9.19	-	9.19	-
0.2	8.64	5.9	4.22	54.0
0.4	6.97	24.1	3.34	63.6
0.6	4.90	46.6	2.02	77.9
0.8	3.81	58.5	1.46	84.0
1.0	2.88	68.6	1.36	85.2

By comparing the inhibition efficiencies of 2PCOX and 3PCOX, 3PCOX was showing efficiency 54% at a concentration of 0.2mM, but in the case of 2PCOX for the same concentration got only 5.9% efficiency. Even at lower concentrations, a noticeable value of η_W % was obtained for 3PCOX on carbon steel specimens, suggesting that the oxime molecules are fairly adsorbed on the metal surface.

Adsorption isotherm and free energy of adsorption

The mechanism of adsorption and the surface behavior of organic molecules can be easily viewed through adsorption isotherms. Different adsorption isotherms considered are Langmuir, Temkin, Frumkin, El- Awady, Flory-Huggin and Freundlich isotherms. For the evaluation of thermodynamic parameters it is necessary to determine the best fit isotherm with the aid of correlation coefficient (R^2). Among the isotherms mentioned above, the best description of the adsorption behavior of 2PCOX and 3PCOX on carbon steel specimens in 1.0M HCl was El-Awady and Langmuir adsorption isotherm respectively which can be expressed as

El-Awady adsorption isotherm $\log(\theta/1-\theta) = \log K + y\log C$ (6)

Langmuir adsorption isotherm $\frac{C}{\theta} = \frac{1}{K_{ads}} + C$ (7)

where C is the concentration of the inhibitor, θ is the fractional surface coverage and K_{ads} is the adsorption equilibrium constant [15].

Among the various adsorption isotherm tried the most suitable one was selected with the help of regression coefficient. **Table 2** contains the adsorption isotherm and their regression coefficients for 2PCOX and 3PCOX on carbon steel in 1.0M HCl. **Figure 3a** and **3b** represents the adsorption isotherm plots of 2PCOX and 3PCOX obtained by the weight loss measurements of carbon steel specimens in 1.0M HCl at 28 ^{0}C.

Table 2 Adsorption isotherm and their regression Coefficients for 2PCOX and 3PCOX on in 1.0M HCl

Adsorption isotherm	Regression coefficient	
	2PCOX	**3PCOX**
Langmuir	0.555	0.992
Freundlich	0.975	0.922
Frumkin	0.973	0.990
Temkin	0.980	0.965
El-Awady	0.996	0.956
Flory-Huggin	0.547	0.913

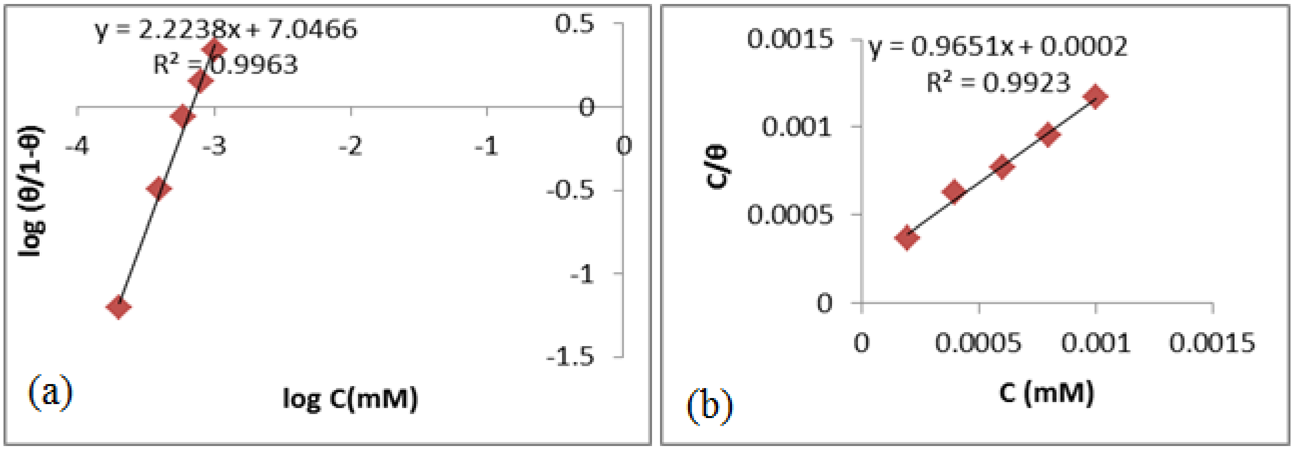

Figure 3 (a) El-Awady adsorption isotherm for 2PCOX on CS surface in 1.0M HCl at 28 ^{0}C. (b) Langmuir adsorption isotherm for 3PCOX on CS surface in 1.0M HCl at 28 ^{0}C

The adsorption equilibrium constant K_{ads} is related to the standard free energy of adsorption ΔG^0_{ads}, by

$$\Delta G^0_{ads} = -RT\ln(55.5\ K_{ads}) \qquad (8)$$

Where 55.5 is the molar concentration of water, R is the universal gas constant and T is the temperature in Kelvin [16]. **Table 3** explores thermodynamic parameters obtained from weight loss measurements of CS specimens in 1.0M HCl. ΔG^0_{ads} for 2PCOX and 3PCOX on CS showed negative values indicating the spontaneity of the process. The value of ΔG^0_{ads} up to -20kJ mol^{-1} is an indication of the electrostatic interaction of the charged molecule and the charged surface of the metal (physisorption) while ΔG^0_{ads} value more negative than -40kJ implies that inhibitor molecules are adsorbed strongly on the metal surface through co-ordinate type bond (chemisorption) [16-18]. In the present investigation, 2PCOX and 3PCOX molecules showed ΔG^0_{ads} -28.32 and -32.4 respectively for CS specimens suggesting that the adsorption of molecules involve both electrostatic adsorption and chemisorption.

Table 3 Thermodynamic parameters obtained from adsorption of oximes

Inhibitor	**K_{ads}**	**ΔG^0_{ads} (kJ/mol)**
2PCOX	1477	-28.32
3PCOX	5000	-31.4

EIS measurements

The corrosion response of carbon steel in 1.0M HCl in the presence and absence of inhibitor has been investigated using Electrochemical Impedance Spectroscopy at 28^0C. **Figure 4** represent the Nyquist plots of 2PCOX and 3PCOX on carbon steel specimens in 1.0M HCl respectively. It is evident from the plots that the impedance response of metal specimens showed a marked difference in the presence and absence of the inhibitors.

The semicircles observed to be depressed to the z' (real) axis or showed slight irregularity which may be attributed to the roughness or non homogeneous nature of the metal surface [19-22]. The capacitance loop intersects the real axis at higher and lower frequencies. The intercept, at high frequency end, corresponds to the solution resistance (R_s) and at lower frequency end, corresponds to the sum of solution resistance (R_s) and charge transfer resistance (R_{ct}). The value of R_{ct} is a measure of electron transfer across the exposed area of the metal surface and it is inversely proportional to rate of corrosion [23].

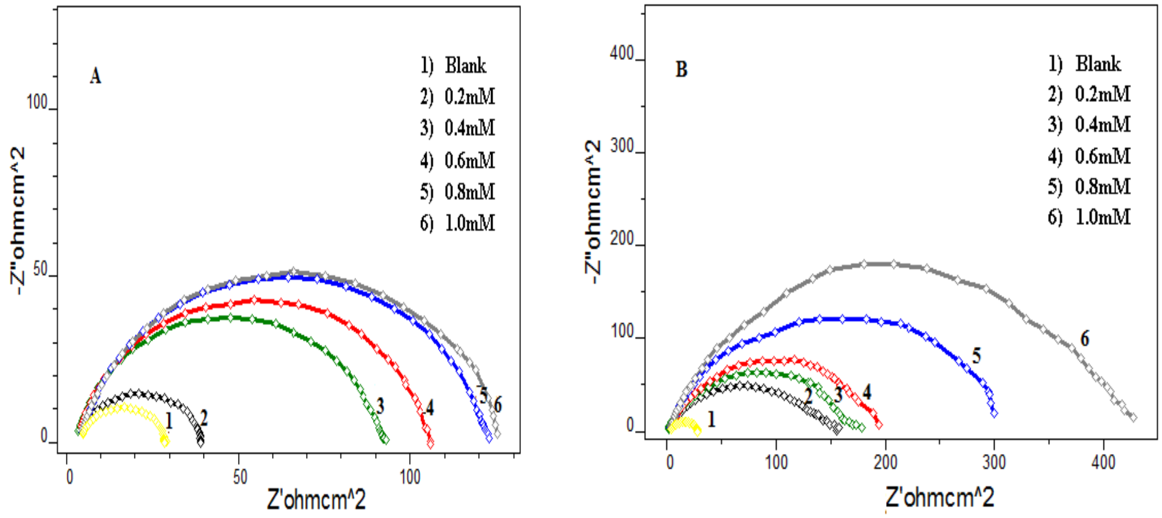

Figure 4 Nyquist plots for CS specimens in 1.0M HCl in the presences and absence of (A) 2PCOX and (B) 3PCOX

Impedance behavior can be well explained by pure electric models that could verify and enable to calculate numerical values corresponding to the physical and chemical properties of electrochemical system under examination [24]. The simple equivalent circuit, that fit to many electrochemical system is composed of a double layer capacitance, R_s and R_{ct} [5, 25, 26]. To reduce the effects due to surface irregularities of metal, constant phase element (CPE) is introduced into the circuit instead of a pure double layer capacitance which gives more accurate fit as shown in the **Figure 5** [27].

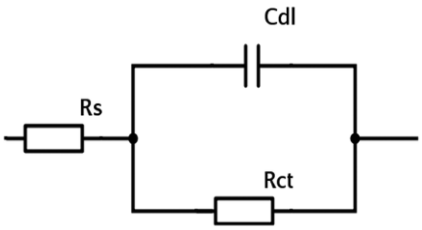

Figure 5 Equivalent circuit fitting for EIS measurements

The impedance of CPE can be expressed as

$$Z_{CPE} = \frac{1}{Y_0 \quad (j\omega)^n} \qquad (9)$$

Where, Y_0 is the magnitude of CPE, n is the exponent (phase shift), ω is the angular frequency and j is the imaginary unit. CPE may be resistance, capacitance and inductance depending upon the values of n [5]. In all experiments the observed value of n ranges between 0.8 and 1.0, suggesting the capacitive response of CPE. The EIS parameters such as R_{ct}, C_{dl} and the calculated values of percentage of inhibition (η_{EIS}%) on CS specimens of 2PCOX and 3PCOX are listed in **Table 4**.

Table 4 Electrochemical impedance parameters of CS specimens, in 1.0M HCl at 28^0C, in the absence and presence of 2PCOX and 3PCOX

Inhibitor	Conc. (mM)	C_{dl} (μFcm^{-2})	R_{ct} (Ωcm^2)	η_{EIS}%
	Blank	90.5	22.7	-
2PCOX	0.2	67.8	32.4	29.7
	0.4	79.9	83.6	72.8
	0.6	57.6	95.9	76.2
	0.8	105.0	110.7	79.4
	1.0	83.1	113.2	79.8
3PCOX	0.2	84.5	125	81.8
	0.4	147.0	147.3	84.5
	0.6	66.1	153.4	85.1
	0.8	103.8	265.9	91.4
	1.0	98.6	381.7	94.0

From Table 4, it is clear that R_{ct} values are increased with increase in inhibitor concentration. Capacitance values C_{dl} can be attributed to the local dielectric constant or the thickness of the electrical double layer. This emphasized the action of inhibitor molecules by adsorption at the metal–solution interface [28]. In both cases the percentage of inhibition (η_{EIS} %) showed a regular increase with increase in inhibitor concentration. A maximum of 94% inhibition efficiency could be achieved at an inhibitor concentration of 1mM for 3PCOX. The $\eta_{EIS\%}$ data reveal that the corrosion inhibition capacity of 3PCOX is comparatively greater than 2PCOX at all concentration, which may be attributed to the high rate of desorption of the inhibitor molecules from the metal surface.

Potentiodynamic polarization studies

Polarization parameters like corrosion current densities (I_{corr}), corrosion potential (E_{corr}), cathodic Tafel slope (b_c), anodic Tafel slope (b_a), and inhibition efficiency (η_{EIS}%) of 2PCOX and 3PCOX on CS specimens are listed in **Table 5a** and **5b** respectively. A prominent decrease in the corrosion current density (I_{corr}) was observed in the presence of 2PCOX. A lowest value of I_{corr} was noticed for the 2PCOX concentration 1mM, and exhibited a maximum inhibition efficiency of 79.6%.

Table 5a Potentiodynamic polarization parameters of CS specimens in 1.0M HCl at 28 ^{0}C in the absence and presence of 2PCOX

Conc.	Tafel Data					Linear polarization data	
(mM)	E_{corr} (mV/SCE)	I_{corr} (μA/cm^2)	b_a (mv/dec)	-b_c (mV/dec)	η_{pol}%	R_p (ohm)	η_{Rp}%
0	-460	796	108	178	-	47.6	-
0.2	-459	662	103	192	16.8	56.7	16.0
0.4	-478	248	103	145	68.8	165	71.2
0.6	-399	190	89	143	76.1	195	75.6
0.8	-461	152	82	140	80.9	224	78.8
1.0	-399	137	80	130	82.8	233	79.6

Table 5b Potentiodynamic Polarization parameters of CS specimens in 1.0M HCl at 28^0C in the absence and presence of 3PCOX

Conc.	Tafel Data					Linear polarization data	
(mM)	E_{corr} (mV/SCE)	I_{corr} (μA/cm^2)	b_a (mV/dec)	-b_c (mV/dec)	η_{pol}%	R_p (ohm)	η_{Rp}%
0	-460	796	108	178	-	47.6	-
0.2	-476	135	90	157	83	177	73.1
0.4	-479	127	78	140	84	213	77.7
0.6	-527	94	77	133	88.2	230	79.3
0.8	-442	56	73	148	93	417	88.3
1.0	-525	34	62	130	96	444	89.6

The corrosion potential (E_{corr}) of the metal specimen was not changed appreciably during the experiment. Since the anodic Tafel slope b_a and cathodic Tafel slope b_c of the inhibited solutions were not changed appreciably from the anodic and cathodic slopes of uninhibited solutions, the inhibitor 2PCOX can be considered as a mixed type inhibitor. Generally if the shift of E_{corr} is >85 with respect to E_{corr} of uninhibited solution, the inhibitor can be viewed as cathodic or anodic type [18, 27, 28]. In the present study the maximum shift of E_{corr} is less than 85mV, suggesting that 2PCOX acts as a mixed type inhibitor for carbon steel specimens in 1.0MHCl. Potentiodynamic polarization curves for CS in the absence and presence 2PCOX and 3PCOX in 1.0M HCl are shown in **Figure 6A** and **B** respectively.

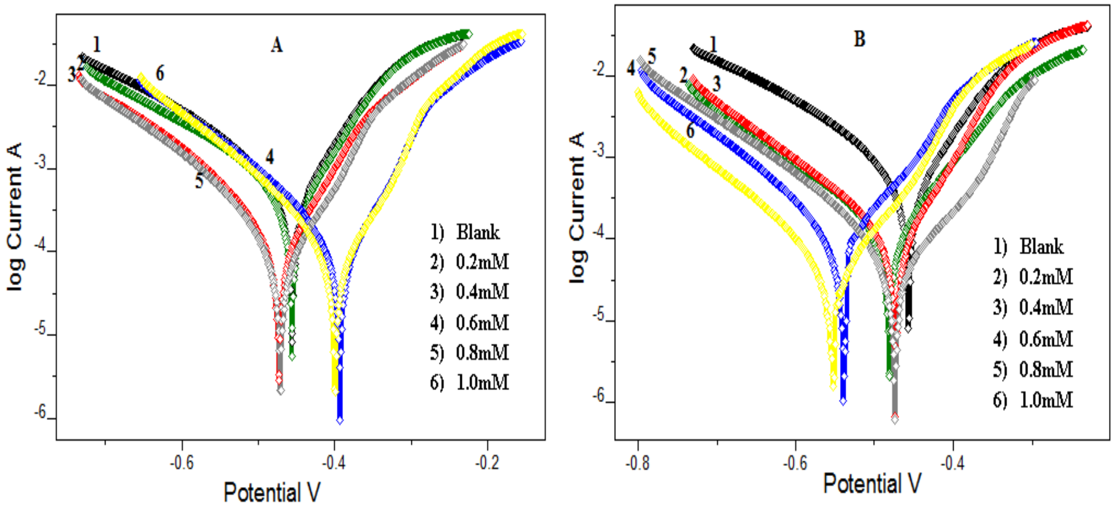

Figure 6 Tafel plots for CS specimens in the presence and absence of the inhibitor (A) 2PCOX and (B) 3PCOX

Electrochemical polarization analysis of 3PCOX on carbon steel specimens also showed a gradual decrease in the corrosion current densities. Both anodic slopes (b_a) and cathodic slope (b_c) do not change appreciably in the case of 3PCOX, which clearly establish that 3PCOX also act as mixed type inhibitor. According polarization studies the maximum inhibition efficiency obtained for 3PCOX was 96.9%, at 1mM concentration. Polarization studies also revealed that, high inhibition efficiencies are obtained for 3PCOX compared to the inhibition efficiencies for 2PCOX at all concentration.

Mechanism of Inhibition

The lower corrosion inhibition efficiency of 2PCOX compared to that of 3PCOX can be explained as follows. When examine the structures of the molecules, one can predict the possibility of formation of hydrogen bonds. 2PCOX prefer to make intra molecular hydrogen bond while 3PCOX molecules largely aggregate by inter molecular hydrogen bonds. It is well known that the surface interaction by the molecules on the metal is the main factor responsible for the mitigation of the rate of corrosion. If 2PCOX form intra molecular hydrogen bonds, it can be assumed that the molecules interact the metal surface independently i.e., there is no molecular interaction between the adsorbed molecules. Protons have thus an ample opportunity to attack on the metal surface as depicted in **Figure 7A**. If we consider the intermolecular hydrogen bond in 3PCOX molecules, we can assume that molecular layers adsorbed on the iron surface appreciably. The exposed area of the metal towards the corroding medium will be significantly reduced due to this phenomenon Figure 7B. Thus the rate of corrosion is appreciably lowered due to the capacity of 3PCOX to make inter molecular hydrogen bonds.

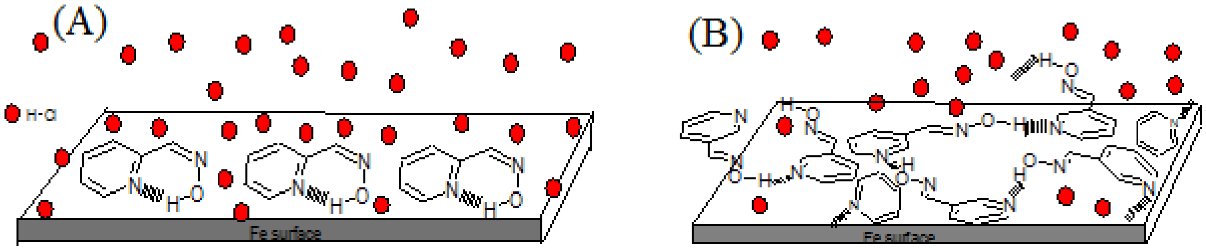

Figure 7 (A) Interaction of 2PCOX on carbon steel in 1.0M HCl, (B) Interaction of 3PCOX on carbon steel in 1.0M HCl

If one examines the structure of oxime, many potential sources of inhibitor–metal interaction can be recognized. The unshared pair of electrons present on two N atoms is of key importance in making coordinate bond with the metal. The π-electron cloud of the aromatic rings and the azomethine linkage also participate in the inhibition mechanism. Furthermore, the double bonds in the inhibitor molecule permit the back donation of metal d electrons to the π* orbital and this type of interaction cannot occur with amines [29].

Conclusions

- For the oximes 2PCOX and 3PCOX a maximum of 82.8% and 96% of inhibition efficiency respectively shown by Tafel studies.
- Corrosion inhibition efficiency of the oximes 2PCOX and 3PCOX are in good agreement with weight loss measurement, EIS studies and potentiodynamic polarization studies.
- Among oximes, 3PCOX exhibited higher corrosion inhibition efficiency than 2PCOX at all concentrations.
- The inhibition mechanism was well explained by adsorption isotherms. Adsorption of 2PCOX and 3PCOX on carbon steel surface obey El-Awady and Langmuir adsorption isotherm respectively.
- The thermodynamic parameters of adsorption were calculated from the adsorption isotherms which showed that both physisorption and chemisorption are involved in the inhibition process.

Acknowledgement

Authors are grateful to University Grant Commission, New Delhi for providing financial support.

References

[1] F. Bentiss, M. Traisnel, L. Gengembre, M. Lagrenée, Appl. Surf. Sci., 2000,161,194.
[2] A. Raman, P. labine, Reviews on Corrosion Inhibitor Science and Technology, NACE, Houston, TX, 1986, 1.
[3] E.E. Oguzie, Mater. Lett., 2005, 59, 1076.
[4] Aysel Yurt, Özlem Aykın, Corros. Sci., 2011, 53, 3725.
[5] Ashish Kumar Singh, Sudhish Kumar Shukla, Manjeet Singh, M.A. Quraishi, Mater. Chem. Phy., 2011, 129, 68.
[6] M. Behpour, S.M. Ghoreishi, N. Soltani, M. Salavati-Niasari, M. Hamadanian, A. Gandomi, Corros. Sci., 2008, 50, 2172.
[7] K.Stanly Jacob, Geetha Parameswaran, Corros. Sci., 2010, 52, 224.
[8] A. Paul, K. J. Thomas, V. P. Raphael, K. S Shaju, Orient. J. Chem., 2012, 28 (30), 1501.
[9] V. P Raphael, K. J Thomas, K. S Shaju, A.Paul, Res. Chem. Intermed., 2014, 40(8), 2689.
[10] A. Bansiwal, P. Anthony, S.P. Mathur, Br. Corros. J., 2000, 35(4), 301.
[11] Shulan Li, Shenhao Chen, Shengbin Lei, Houyi Ma, Rui Yu, Dexin Liu, Corros. Sci., 1999, 41, 1273.
[12] AST G-31-72, Standard recommended practice for the laboratory immersion corrosion testing of metals, ASTM, Philadelphia, PA, 1990.
[13] H. Ashassi-Sorkhabi, B. Shaabani, D. Seifzadeh, Electrochim. Acta., 2005, 50, 3446.
[14] I.B. Obot, N.O. Obi-Egbedi, Corrs. Sc., 2010, 52,198.
[15] Xianghong Li, Shuduan Deng, Hui Fu, Taohong Li, Electrochim. Acta., 2009,54,4089.
[16] E. Cano, J.L. Polo, A. La Iglesia, J.M. Bastidas, Adsorption, 2004, 10,219.
[17] F. Bentiss, M. Lebrini, M. Lagrenée, Corros. Sci., 2005, 47, 2915.
[18] Wei-hua Li, Qiao He, Sheng-tao Zhang, Chang-ling Pei, Bao-rong Hou, J. Appl. Electrochem., 2008, 38, 289.
[19] Hamdy H. Hassan, Essam Abdelghani, Mohammed A. Amin, Electrochim. Acta., 2007, 52, 6359.
[20] M.S. Abdel-Aal, M.S. Morad, Br. Corros. J., 2001, 36, 253.
[21] P. Bommersbach, C. Alemany-Dumont, J.P. Millet, B. Normand, Electrochim. Acta., 2005, 51,1076.
[22] F.Mansfeld, Corrosion, 1981, 36, 301.
[23] I.L. Rosenfield, Corrosion Inhibitors, McGraw-Hill, New York, 1981.
[24] A.S.Priya, V.S. Muralidharam, A.Subramannia, Corrosion, 2008, 64,541.
[25] M. El Azhar, B. Mernari, M. Traisnel, F. Bentiss, M. Lagrenée, Corros. Sci., 2001, 43, 2229.
[26] A. Yurt, A. Balaban, S.Ustün Kandemir, G. Bereket, B. Erk, Mater. Chem. Phys., 2004, 85, 420.
[27] Q. Qu, Z. Hao, S. Jiang, L. Li, W. Bai, Mater. Corros., 2008, 59, 883.
[28] F. Bentiss, M. Traisnel, M. Lagrenee, Corros. Sci., 2000, 42, 127.

[29] D. Paul Schweinsberg, Graeme A. George, Asanka Kuruppu Nanayakkara, Dale A. Steinert, Corros. Sci., 1988, 28, 33.

Publication History

Received	22nd Oct 2017
Revised	08th Nov 2017
Accepted	10th Nov 2017
Online	30th Nov 2017